Zr-shift at the origin of the exceptional piezoelectric properties of $PbZr_{0.52}Ti_{0.48}O_3$

A. Al-Zein,[1,2] G. Fraysse,[1] J. Rouquette,[1,*] Ph. Papet,[1] J. Haines,[1] B. Hehlen,[2] C. Levelut,[2] G. Aquilanti,[3] and Y. Joly[4]
[1]*Institut Charles Gerhardt Montpellier, UMR CNRS 5253, équipe C2M, Université Montpellier II, 34095 Montpellier Cedex 5, France*
[2]*Laboratoire des Colloïdes, Verres et Nanomatériaux (LCVN), UMR CNRS 5587, Université Montpellier II, 34095 Montpellier Cedex 5, France*
[3]*European Synchrotron Radiation Facility, 6 rue Jules Horowitz, BP 220, 38043 Grenoble Cedex 09, France*
[4]*Institut Néel, CNRS, Université Joseph Fourier, BP 166, 38042 Grenoble Cedex 9, France*
(Received 13 April 2010; published 12 May 2010)

In spite of intensive experimental and theoretical studies, no model at the atomic scale has been proposed to explain the large piezoelectric effect in $PbZr_{0.52}Ti_{0.48}O_3$ (PZT) compared to the low piezoelectric response in the simple end-member lead titanate $PbTiO_3$. X-ray absorption spectroscopy (XAS) appears as the technique of choice not only to clarify the role of Zr, but also to quantify the Zr displacement through the Ferroelectric-Paraelectric (*F-P*) transition. We clearly show evidence of the polar character of the Zr-atoms in PZT with a Zr-shift which will produce a small polarization. Such an atomic configuration for one type of atoms leads to relatively easy switching, i.e., relatively low electric field to align the Zr-polar atoms, which will create a favorable energetic situation for the cooperative switching of the strongly polar Ti-O dipole and would therefore account for the large piezoelectric effect in PZT.

DOI: 10.1103/PhysRevB.81.174110 PACS number(s): 77.65.−j, 61.05.cj, 61.50.Ks, 77.84.Cg

I. INTRODUCTION

Understanding the physical behavior of a material at the atomic scale has always presented a great challenge to condensed matter physicists and materials scientists. The effort to elucidate the role played by Zr/Ti atoms which are at the origin of the polar displacements in ferroelectric $PbZr_{0.52}Ti_{0.48}O_3$ (PZT) is a prime example of such a challenge.[1–3] PZT exhibits a *F-P* phase transition at a critical temperature T_C (and a critical pressure P_C), which can be defined from a structural point of view as a phase transition from a noncentrosymmetric to a centrosymmetric structure and due to the disappearance of the spontaneous polarization characterizing these materials,[4] Fig. 1. The origin of the large dielectric susceptibility and piezoelectric properties in these highly polarizable ferroelectric perovskite of general formula ABO_3 is due to the cooperative displacement of the *B* cations, i.e., the Zr/Ti atoms in our case [Fig. 1(a)], from the center of symmetry of their octahedral sites below a critical temperature T_C (and critical pressure P_C). These spontaneous displacements create local dipoles that are aligned parallel one to another in order to give a macroscopic dipole moment by application of an electric field *E*.

PZT is widely used in technological applications due to its high piezoferroelectric properties. This particular composition, i.e., $x=0.48$ in the $Pb(Zr_{1-x}Ti_x)O_3$ solid solution, exhibits the highest electromechanical response and is generally termed as the morphotropic phase boundary (MPB) separating the Zr-rich rhombohedral from the Ti-rich tetragonal phase.[5] Recently, the MPB has attracted particular attention due to the discovery of a monoclinic phase (*Cm*) in this compositional range at temperatures below 300K.[6] In the paraelectric form (above $T_C=664$ K), PZT is cubic with a Pb atom at each corner of the cubic lattice, the Ti/Zr atoms in the center and the oxygen atoms are at the centers of the faces, Fig. 1(b). Upon decreasing temperature, both Pb and Ti/Zr will move along the pseudocubic [001] direction giving rise to the tetragonal form, Fig. 1(a). As PZT is a ferroic material, it exhibits domain configurations (elastic and electric) which make the understanding of these compounds much more complex. Different scales should be taken into account: from the atomic scale (individual polar displacements) to the macroscopic scale (macroscopic piezoelectric effect) and finally the mesoscopic scale in between which is governed by the domain wall motion. High piezoelectric properties (PZT, PMN, PZN) are structurally linked to strong disorder which can be characterized by the presence of diffuse scattering[7–9] in diffraction experiments and by nanosized domains.[10] In this XAS study and due to the experimental technique used, we only focused on the characterization of the Zr-polar displacements at the atomic scale. In PZT, the role of Pb atoms is of particular importance as it hybridizes with oxygen states leading to a large

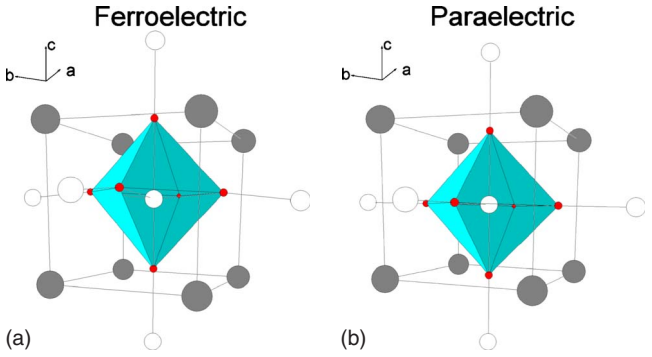

FIG. 1. (Color online) (a) Ferroelectric state with a tetragonal ($P4mm$) crystal structure and (b) paraelectric state with a cubic ($Pm\bar{3}m$) crystal structure. Pb atoms (gray) at each corner of the pseudocubic lattice with Ti/Zr (white) in the center. Oxygen atoms (red) are at the center of the faces. In the ferroelectric form below T_C or P_C, both Pb and Ti/Zr will have atomic displacements along [001] giving rise to the spontaneous polarization. The spontaneous polarization disappears in the paraelctric form above T_C or P_C.

strain.[1] Since the only difference between $PbTiO_3$ end-member (d_{33}=35 pC/N) (Ref. 11) and $PbZr_{0.52}Ti_{0.48}O_3$ (d_{33}=520 pC/N) (Ref. 12) is the presence of zirconium, we focus our study on the role of the Zr atom in PZT solid solutions to understand this difference in the piezoelectric constants. The $3d^0/4d^0$ state of the Ti/Zr atoms can give an insight to the local shifts on the same site, i.e., the center of the oxygen octahedron. Zr^{4+} and Ti^{4+} have ionic radii of 0.72 and 0.605 Å, respectively.[13] One can therefore expect a much more pronounced off-center shift of smaller Ti atoms in their oxygen octahedra cage in comparison to the larger Zr atoms. This scenario was confirmed based on XAS (Ref. 14) and pair distribution function measurements;[15] the Ti off-center displacement is experimentally found to be about 0.2–0.3 Å, while Zr is found to have either a small shift (0.07 Å) (Ref. 14) or no shift.[15] Additionally, although the Zr shift is found to be both temperature and composition independent,[14,16] the Ti shifts appear to have an order-disorder component as a function of temperature[17] and pressure[18] which was found to be quite unusual for these ferroelectric displacive-type transitions.[19] This paper provides the evidence of the ferroelectric character of the Zr-atoms in PZT in the *P-T* space. The small Zr shifts (0.06 Å) are found to disappear with a small order-disorder component above the ferroelectric-paraelectric transition based on (i) the behavior as a function of pressure of the EXAFS Debye-Waller factor (DWF) σ^2 which accounts for the disorder in the Zr-O distance and (ii)-the smooth decrease in intensity of the pre-edge fine structure (PEFS) which is associated with the loss of the dipolar contribution.

II. EXPERIMENTAL

Zr *K* edge measurements (17998 eV) at high pressure and high temperature were performed in transmission geometry at beamline BM29 of the European Synchrotron Radiation Facility. A (311) Si monochromator with a resolution of 0.5 eV was used. A Paris-Edinburgh press, equipped with sintered diamond anvils and 5 mm boron/epoxy biconical gaskets with a high x-ray transmission in the selected energy range were used. A finely ground powder of $PbZr_{0.52}Ti_{0.48}O_3$ was mixed with boron nitride used as light element matrix and known to be chemically inert to the materials, in order to have the appropriate sample thickness for XAS measurements. The sample-matrix mixture was pelleted to a cylindrical shape, inserted into boron nitride capsule itself inserted in a graphite furnace and finally placed into the gasket. Note that the use of boron nitride capsule was necessary in order to avoid the reduction of PZT by graphite at high temperature. In order to characterize the sample and to measure the *P* and *T* data, a monochromatic beam (20 keV) was impinged onto the sample and the diffraction rings from the sample were intercepted by a MAR345 image plate detector mounted in an offset position. This *in situ* diffraction measurement has also enabled us to check the tetragonal distortion of PZT in *P-T* space. XAS data were collected in transmission mode each 1–2 GPa along 2 isotherms (300 K, 450 K). The EXAFS data analysis was carried out with the IFEFFIT package.[20] The contribution of interest to the total

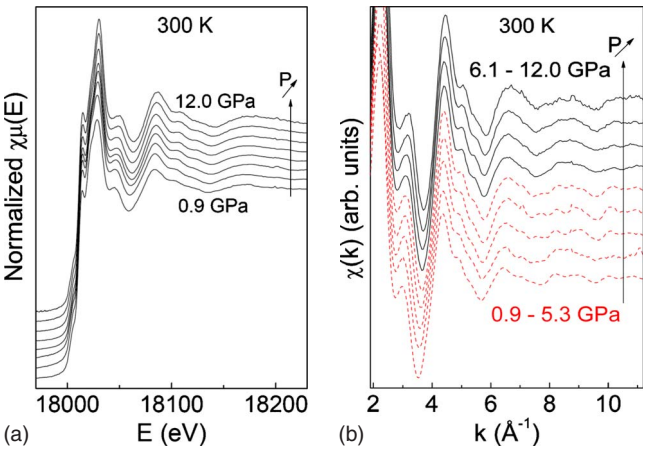

FIG. 2. (Color online) (a) Normalized XAS spectra obtained at 300 K between 0.9 GPa and 12 GPa, (b) Extracted $\chi(k)$. Both signals are vertically shifted for clarity.

EXAFS signal is given by the single scattering between the photoabsorber and the first six neighbors, i.e., the Zr-atoms and the six oxygen octahedra in the whole pressure range.

At low photoelectron energy, single scattering or path expansion are not sufficient to simulate the experiments. Better techniques, such as the full multiple scattering theory are thus required. For the XANES part of the spectra we used the FDMNES code[21] using the finite difference method with the full multiple scattering theory. We chose in this study this theory which works within the muffin-tin approximation on the potential shape, but is more tractable with large systems. The PEFS are caused by the unoccupied *p* and *d* states of the *B* atoms in the perovskite.[22] For an absorbing atom out of a center of symmetry, an increased dipolar contribution associated to the hybridization of the *d* and *p* states appears in the intensity at the pre-edge. The intensity of this peak is a direct measurement of the polar shift. This implies that in the paraelectric form only the quadrupolar contribution can be observed.

III. RESULTS AND DISCUSSION

High quality, high-pressure XAS data of PZT were normalized to the jump at the absorption edge and the apparent small effect of pressure on the Zr *K* edge spectra can be seen, Fig. 2(a). Namely, the extracted $\chi(k)$ spectra, Fig. 2(b), evidence above 6.1 GPa a disappearance of some high frequency contributions: in particular the split doubled features between k=6 $Å^{-1}$ and k=7.5 $Å^{-1}$ and between k=8 $Å^{-1}$ and k=10 $Å^{-1}$ merge into two single oscillations respectively. Based on these data, there might be a low-pressure behavior below ~6.1 GPa, and a high-pressure behavior above.

In Fig. 3(a), we show Fourier transforms of the EXAFS signal at 3.7 GPa and 7.0 GPa, first peak of which can be correlated with the radial distribution function around the photoabsorber. At 7.0 GPa, the maximum of the peak is shifted with respect to that at 3.7 GPa indicating a weak contraction of the Zr-O distance and the peak amplitude is higher. Nonetheless the shape of the first peak of the Fourier

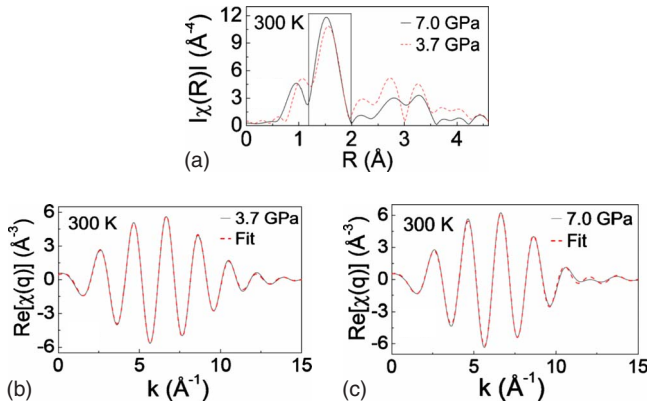

FIG. 3. (Color online) (a) The k^3-weighted EXAFS signals (obtained in the 2–11 Å^{-1} range) are shown at 3.7 GPa (dashed) and 7.0 GPa (full). The Zr-O first coordination shell is extracted using a Hann window in the 1.2–2 Å range. (b) and (c) The k^3-weighted backward Fourier transforms along with the resulting fits (dashed) are shown at 3.7 and 7 GPa, respectively.

transform is a Gaussian at all pressures allowing us to use the same structural model given by six oxygen atoms as first neighbors at the same distance. The fitting was done in q space isolating the Zr-O peak of the Fourier transform and the back transforming in q space using a standard procedure. A symmetric distribution of bond distances was used, characterized by the following structural parameters: R (average bond distance), σ^2 [relative mean square displacement or EXAFS DWF: $\exp(2\sigma^2k^2)$], and the number of neighbors which was kept fixed to six. Figures 3(b) and 3(c) show the Zr-O atom pair distribution function, i.e., backward Fourier transform, in the k^3-weighted space along with the best fit calculation obtained at 3.7 and 7 GPa. The experimental data are correctly reproduced within the pressure range of investigation.

Figure 4 shows the pressure behavior of the experimental σ^2 for the Zr-O atom pairs at 300 K; σ^2 accounts for the mean square displacement of the Zr-O distance and contains two contributions: a thermal ($\sigma^2_{dyn.}$) and a structural ($\sigma^2_{stat.}$) contribution linked to the local vibrational dynamics and the local structural distortions, respectively. One can first note that the fitted ambient value is perfectly consistent with that reported in the literature[14] (the open star). Additionally, a noticeable decrease of σ^2 can be observed with increasing pressure with a change in the trend at ~7 GPa.

To interpret these data, it is important to compare them with the σ^2 of centrosymmetric Zr-based oxide compounds. Since the $PbZrO_3$ end member is antiferroelectric, it will have antiphase polar displacements. Additionally, it was found that its structure is disordered with two substructure components related by a shear of $c/2$.[23] In our study, $BaZrO_3$ (BZ) was chosen because the Zr atoms are known to be perfectly in the center of the oxygen octahedra in the whole pressure-temperature range,[24] implying that the σ^2 in BZ is only dependent on the thermal vibrations (θ_E=606 K) and does not contain the static contribution.[25] Note that other centrosymmetric Zr-based oxide materials [for example, ZrW_2O_8 (Ref. 25)] also exhibit similar values of σ^2.

The behavior of $\sigma^2_{dyn.}$ (BZ) at a fixed temperature (300 K) can be expected to smoothly decrease upon increasing pressure. This decreasing behavior of $\sigma^2_{dyn.}$ [dotted line in Fig. 2(d)] can be estimated using the equivalent isotropic temperature factors of the B atom reported in a high-pressure single crystal diffraction study[26] of $GdFeO_3$, a centrosymmetric perovskite (no static disorder) which exhibits no phase transition in the pressure range of interest. The pressure dependence of $\sigma^2_{dyn.}$ corresponds to a decrease of about 1% per GPa.[26]

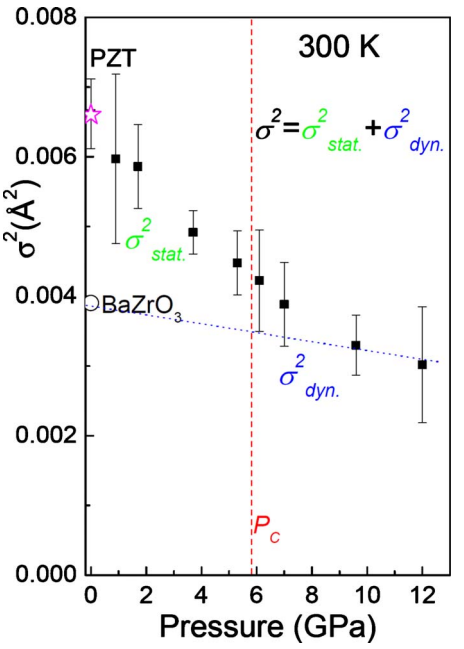

FIG. 4. (Color online) Pressure behavior of the DWF for the Zr-O atom pairs at 300 K. Values reported in the literature for PZT (Ref. 14) (∗) and $BaZrO_3$ (Ref. 24) (○) are also included. P_C (the dashed line) corresponds to the paraelectric transition (Ref. 9). The dotted line represents the decrease of $\sigma^2_{dyn.}$ as explained in the text.

At ambient conditions, we can observe that the σ^2 of PZT is higher than that of BZ, this can be attributed to the presence of static disorder in PZT, which is absent in BZ. At high pressure, the $\sigma^2_{dyn.}$ estimation of BZ perfectly fits the high-pressure values of σ^2 for PZT indicating that pressure eliminates the static disorder for the Zr-atoms of PZT above 7 GPa and that the only contribution to the EXAFS DWF is dynamic above this pressure. Based on previous studies, we have already characterized the ferroelectric-paraelectric phase transition of PZT at 5–6 GPa,[9] Fig. 4 (P_C: dashed line). This phase transition can be linked to the change in the decrease in σ^2 for the Zr-O bond and the situation (low-pressure regime) in which the EXAFS DWF contains the static and dynamic contributions and that (high-pressure regime) in which only the dynamic part contributes to the σ^2. This implies that $\sigma^2_{stat.}$ of PZT is due to a small random Zr off-center displacement in the oxygen octahedra cage, which will produce a small polarization. This Zr-shift can be roughly estimated ~0.06 Å, i.e., $\sqrt{0.0067-0.003} \cong 0.06$ Å. The excess of $\sigma^2_{stat.}$ appears at pressures well above P_C suggesting an order-disorder nature of the transition, as it has already been reported for Ti shifts in P-T space.[17,18] It is worth to stress that besides the displacement of Zr from the offset position to the centrosymmetric position of 0.06 Å,

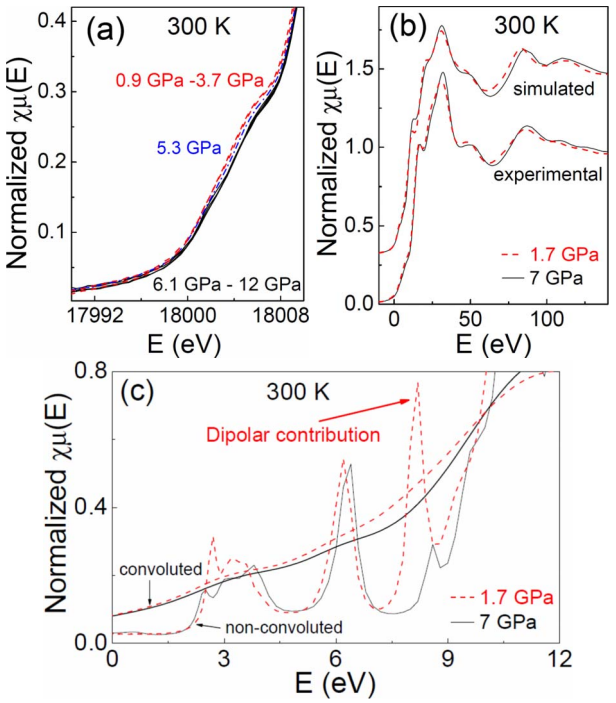

FIG. 5. (Color online) (a) High-pressure Zr *K* edge XANES spectra obtained at 300 K. Note the pressure evolution of the PEFS. (b) Experimental and simulated XANES spectra at 1.7 and 7 GPa. In b), the origin (0) corresponds to the Zr *K* edge. (c) The nonconvoluted and convoluted theoretical PEFS at 1.7 and 7 GPa showing the disappearance of the dipolar contribution at high pressure.

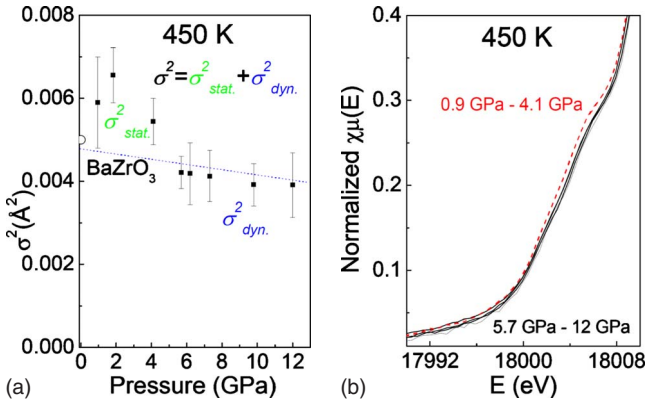

FIG. 6. (Color online) (a) Pressure behavior of the DWF for the Zr-O atom pairs at 450 K. The calculated value for $BaZrO_3$ (○) (Ref. 24) is also included. $\sigma^2_{dyn.}$ (the dotted line) corresponds to a decrease of about 1% per GPa. (b) High-pressure Zr *K* edge XANES spectra obtained at 450 K. Note the pressure evolution of the PEFS.

the average Zr-O distances contract by 0.01 Å indicating the small compressibility of the oxygen octahedra.

Let us now discuss about the XANES part of the spectra. The *p-d* peak, linked to the dipole transition, is expected to disappear at the ferroelectric-paraelectric transition as in $PbTiO_3$. However, it is difficult to observe this effect in PZT (Ref. 16) at Zr *K* edge owing to the large Zr *K* hole width ($\gamma_K(Zr) \approx 3.84$ eV) as compared to that of Ti *K* edge in $PbTiO_3$ [$\gamma_K(\mathrm{Ti}) \approx 0.8$ eV]. The very weak variation of $\sigma^2_{dyn.}$ in this high-pressure experiment enabled us to distinguish a smooth, but observable decrease in the PEFS intensity in the 0.9–6.1 GPa pressure range, as shown in Fig. 5(a). Above 6.1 GPa, the PEFS spectra overlap almost perfectly. The critical pressure for the change in behavior, i.e., 6.1 GPa, is roughly consistent with the results described above, Figs. 2(b) and 4. In order to determine the origin of the change in the behavior in the XANES spectra, we performed full multiple scattering calculations. Based on our structural data obtained from neutron diffraction,[9] an excited atom embedded in a 10 Å cluster was used to simulate the XANES spectra in the ferroelectric and paraelectric state. In the ferroelectric state, a Zr-displacement of 0.06 Å from the symmetric position was kept fixed consistent with the EXAFS results. The theoretical spectra were convoluted with contributions due to the Zr *K* hole width, the photoelectron width and the experimental resolution. Figure 5(b) shows the experimental and simulated XANES spectra obtained at 1.7 and 7 GPa, which are consistent with a long range polar and nonpolar state. All the features are correctly reproduced starting from the more intense white line in the paraelectric state, centered at 30 eV, to the well-known shift to higher energy of the XANES spectrum at high pressure. Note, however, that large convolution with the contribution due to the Zr *K* hole width hides the structure at low energy. We show thus in Fig. 5(c), the nonconvoluted (before broadening) and convoluted spectra at 1.7 and 7 GPa. It is here clearly possible to identify the dipolar contribution in the low-pressure spectrum at about 8.2 eV due to the breaking of the inversion symmetry induced by the small Zr-shift from its symmetric position. At high pressure in the paraelectric state, i.e., 7 GPa, only the quadrupolar contribution for which intensities are only very weakly affected by the Zr shift can be observed. Therefore contrary to what was expected, these simulations confirm that even a small Zr shift can be observed in the PEFS signal. This confirms that XAS measurements are a perfect probe of local polar displacements. Note that for the EXAFS analysis mentioned above, the small Zr shift can only be observed due to the high-pressure measurements at constant temperature. As stated previously, the thermal vibrations in our case are almost constant thereby making the interpretation considerably easier.

Figure 6(a) shows the pressure behavior of the experimental σ^2 for the Zr-O atom pairs at 450 K. As observed at ambient temperature, a noticeable decrease of σ^2 can be observed with increasing pressure followed by a plateau at higher pressures. The calculated value of σ^2 in BZ at 450K is plotted (θ_E=606 K).[25] As in Fig. 4, the $\sigma^2_{dyn.}$ estimation of BZ (dotted line) is inserted and perfectly fits again with the values of σ^2 for PZT at high pressure giving an additional evidence that pressure eliminates the static disorder for the Zr-O bond in PZT above 5 GPa; again the only contribution to the EXAFS Debye-Waller factor above this pressure will be dynamic. As observed previously, $\sigma^2_{stat.}$ of PZT comes from a small random Zr off-center displacement in the oxygen octahedron cage which will produce a small polarization. This finding is supported by the high-pressure XANES spectra obtained at 450 K, Fig. 6(b). It is possible to distinguish a smooth decrease in the PEFS intensity in the 0.9 GPa–5.7

GPa pressure range. Above 5.7 GPa, the PEFS spectra overlap almost perfectly indicating the disappearance of the dipolar contribution as shown by the full multiple scattering calculations mentioned above.

IV. CONCLUSION

To conclude, this XAS study as a function of pressure and temperature provides the first evidence of the polar character of the Zr atoms in PZT with a Zr shift, which will produce a small Zr polarization. This small polarization can therefore be aligned with a modest electric field which would create a favorable energetic situation for the switching of the strongly polar Ti-O dipole and would therefore account for the large piezoelectric effect in PZT. Viewed from the zirconium site, the local configuration is similar to that expected close to T_C in a classical ABO_3 ferroelectric, at which a maximum in the dielectric constant is observed, i.e., the coercitive electric field necessary to switch the polarization drastically decrease. In mixed *B*-cation systems, such local configurations for one type of *B* cations leads to relatively easy switching giving rise to exceptional ferro/piezoelectric properties. It is interesting to note that this MPB composition, which exhibits the highest piezoelectric performances, has a Zr/Ti compositional ratio of 1/1 which would optimize the process described above. Furthermore, we can analyze other ferroelectric materials, which also present high or giant piezoelectric effect, the $PbMg_{1/3}Nb_{2/3}O_3$ (Ref. 27) and $PbZn_{1/3}Nb_{2/3}O_3$ (Ref. 28) systems for example. Looking at the unoccupied or fully occupied *d* orbitals of the Mg/Nb and the Zn/Nb atoms, it is possible to predict similar behavior. Here, the strong dipole will be Nb-O with small Nb^{5+} of 0.64 Å, while the small polarization will be produced by the larger Mg^{2+} or Zn^{2+}, 0.72 and 0.74 Å, respectively.[13] One can clearly expect that the Mg and Zn atom could be easily poled with a modest applied electric field such as the Zr atom in our study providing an effective way to align the Nb-O dipoles. Finally, this result could be an interesting way to predict new ferroelectric materials with optimal ferropiezoelectric properties.

*Corresponding author. Jerome.Rouquette@univ-montp2.fr

[1] R. E. Cohen, Nature (London) **358**, 136 (1992).
[2] I. Grinberg, V. R. Cooper, and A. M. Rappe, Nature (London) **419**, 909 (2002).
[3] A. M. George, J. Iniguez, and L. Bellaiche, Nature (London) **413**, 54 (2001).
[4] M. E. Lines and A. M. Glass, *Principles and Applications of Ferroelectrics and Related Materials* (Clarendon, Oxford, 1977).
[5] B. Jaffe, W. R. Cook, and H. Jaffe, *Piezoelectric Ceramics* (Academic, London, 1971).
[6] B. Noheda, D. E. Cox, G. Shirane, J. A. Gonzalo, L. E. Cross, and S.-E. Park, Appl. Phys. Lett. **74**, 2059 (1999).
[7] K. Hirota, S. Wakimoto, and D. E. Cox, J. Phys. Soc. Jpn. **75**, 111006 (2006).
[8] J. Rouquette, J. Haines, V. Bornand, M. Pintard, Ph. Papet, C. Bousquet, L. Konczewicz, F. A. Gorelli, and S. Hull, Phys. Rev. B **70**, 014108 (2004).
[9] J. Rouquette, J. Haines, V. Bornand, M. Pintard, Ph. Papet, W. G. Marshall, and S. Hull, Phys. Rev. B **71**, 024112 (2005).
[10] K. A. Schönau, L. A. Schmitt, M. Knapp, H. Fuess, R.-A. Eichel, H. Kungl, and M. J. Hoffmann, Phys. Rev. B **75**, 184117 (2007).
[11] S. Takahashi and M. Takahash, Jpn. J. Appl. Phys. **11**, 31 (1972).
[12] X.-h Du, J. Zheng, U. Belegundu, and K. Uchino, Appl. Phys. Lett. **72**, 2421 (1998).
[13] R. D. Shannon, Acta Crystallogr., Sect. A: Found. Crystallogr. **32**, 751 (1976).
[14] D. Cao, I.-K. Jeong, R. H. Heffner, T. Darling, J.-K. Lee, F. Bridges, J.-S. Park, and K.-S. Hong, Phys. Rev. B **70**, 224102 (2004).
[15] W. Dmowski, T. Egami, L. Farber, and P. K. Davies, AIP Conf. Proc. **582**, 33 (2001).
[16] R. V. Vedrinskii, E. S. Nazarenko, M. P. Lemeshko, V. Nassif, O. Proux, A. A. Novakovich, and Y. Joly, Phys. Rev. B **73**, 134109 (2006).
[17] N. Sicron, B. Ravel, Y. Yacoby, E. A. Stern, F. Dogan, and J. J. Rehr, Phys. Rev. B **50**, 13168 (1994).
[18] N. Jaouen, A. C. Dhaussy, J. P. Itié, A. Rogalev, S. Marinel, and Y. Joly, Phys. Rev. B **75**, 224115 (2007).
[19] W. Cochran, Adv. Phys. **10**, 401 (1961).
[20] M. Newville, J. Synchrotron Radiat. **8**, 322 (2001).
[21] Y. Joly, Phys. Rev. B **63**, 125120 (2001).
[22] R. V. Vedrinskii, V. L. Kraizman, A. A. Novakovich, Ph. V. Demekhin, and S. V. Urazhdin, J. Phys.: Condens. Matter **10**, 9561 (1998).
[23] A. M. Glazer, K. Roleder, and J. Dec, Acta Crystallogr., Sect. B: Struct. Sci. **49**, 846 (1993).
[24] C. Laulhé, F. Hippert, J. Kreisel, M. Maglione, A. Simon, J. L. Hazemann, and V. Nassif, Phys. Rev. B **74**, 014106 (2006).
[25] D. Cao, F. Bridges, G. R. Kowach, and A. P. Ramirez, Phys. Rev. Lett. **89**, 215902 (2002).
[26] N. L. Ross, J. Zhao, and R. J. Angel, J. Solid State Chem. **177**, 3768 (2004).
[27] X. Zhao, W. Qu, X. Tan, A. A. Bokov, and Z.-G. Ye, Phys. Rev. B **75**, 104106 (2007).
[28] S. Park and T. R. Shrout, J. Appl. Phys. **82**, 1804 (1997).